Structural Investigation of $(Ad\ II)_{26}$ Fiber, a Novel Bioengineered Material Based on a Viral Spike Protein

D. Blake Gillespie,† Brad L. Thiel,‡ Kimberly A. Trabbic,† Christopher Viney,† and Paul Yager*,†

Molecular Bioengineering Program, Center for Bioengineering, FL-20, and Department of Materials Science and Engineering, FB-10, University of Washington, Seattle, Washington 98195

Received January 14, 1994; Revised Manuscript Received July 7, 1994®

ABSTRACT: The structure of the $(Ad\ II)_{26}$ fiber, a textile fiber spun from a solution of recombinant polypeptide, was examined using several techniques and compared to models from the literature. The polypeptide is based on a sequence derived from a protein from type 2 human adenovirus. Transmission electron microscopy suggests that there are no long range periodic structures in the fibers. Comparison of Raman spectra taken in two fiber orientations indicates that there is about 59% β-sheet and 19% β-turn. Mechanical studies, light microscopy (including birefringence), and Raman data indicate that the polypeptide backbone is at least partially aligned along the fiber axis. The polypeptide in the spun fiber appears to be organized in a manner different from the trimeric β-sheet rods proposed in models of the viral spike protein.

Introduction

Natural protein-based polymers often possess characteristics that surpass those of the most advanced man-made polymers. Conventional polymer synthesis employs single monomer types or relatively simple copolymers, limiting the structural complexity of the materials derived from them. Polymer lengths are polydisperse, and manufacturing conditions are often extreme. By contrast, polypeptides have more than 20 monomer types, can be of precise lengths, and can self-assemble under comparatively mild conditions. Recombinant DNA technology affords complete control over the amino acid sequence and length, and thus the structure of polypeptides. These factors make natural polymers an attractive prospect for the generation of novel materials.

One such novel material has recently been developed by O'Brien *et al.* at DuPont.[1,2] The poor performance of high-strength polymer fibers under compression in composites led the DuPont groups to search for a self-assembling biological system with good intrinsic compressive strength and the potential to be formed into fibers. The candidate biological system was the spike (or fiber) protein from human adenovirus Ad II.[1,2] In the intact virus, the protein assembles into trimers; the rigid rodlike shape of the spike suggested both that it had good compressive strength and that it might be oriented via formation of a nematic liquid crystalline phase. The central portion of the spike polypeptide can be arranged into 21 or 22 very similar segments of 15 residues each.[3] Three genes, the sequences of which were based on the adenovirus spike, were synthesized and expressed.[1,2,4] One of the resultant proteins is the artificial polypeptide Ad II, which consists of 26 repeats of the following 15 amino acid sequence (henceforth $(Ad\ II)_{26}$): $(Ser\text{-}Gly\text{-}Leu\text{-}Asp\text{-}Phe\text{-}Asp\text{-}Asn\text{-}Asn\text{-}Ala\text{-}Leu\text{-}Arg\text{-}Ile\text{-}Lys\text{-}Leu\text{-}Gly)_{26}$

Although the technique used to express the artificial gene results in a product with polydisperse molecular weight, the fibers used in these studies consisted of 26-mers purified to >90% homogeneity.[1] Dissolving $(Ad\ II)_{26}$ in 1,1,1,3,3,3-hexafluoro-2-propanol produces highly birefringent solutions; these solutions, consisting of aligned structures of unknown nature, were used by the DuPont group to spin the fibers used in this study.[1,4]

There are two distinct models in the literature for the assembly of the adenovirus spike protein, as shown in Figure 1. A primary aim of the work described in this paper was to determine whether either of these models accurately reflects the structure of the protein in fibers spun from $(Ad\ II)_{26}$. The first model, developed by Green *et al.*,[3] folds the repeating sequence of the polypeptide into a long cross-β-sheet ribbon, which then assembles into trimeric rods (or "box beams"[1]), as shown in Figure 1A. The trimer twists because of the intrinsic twist of the antiparallel β-sheet. Note that in this structure most hydrogen bonds are within single strands. The orientation of most of the hydrophobic residues toward the inside of the structure contributes to the stability of the trimer.

Stouten *et al.* have recently reported a different model (see Figure 1B).[5] They note that the Green model was developed to accommodate a possible dimeric structure for the viral spike, but that a cross-β-sheet trimeric structure is only 70% of the required length. They propose that the polypeptide chains are more extended and form a true triple helix in which each of the chains is hydrogen bonded to the chains above and below it in discontinuous segments of parallel β-sheets. The strength of this structure is presumably enhanced by the numerous interstrand hydrogen bonds. Note that in the Green model the polypeptide backbones are essentially perpendicular to the 3-fold axis (except for the turn regions), whereas in the Stouten model the backbones are somewhat more inclined toward the axis.

Raman spectroscopy is a powerful tool for determining both the orientation and secondary structure of proteins in fibers. Depending on the nature of the vibrational mode and the orientation of that mode's Raman tensor with respect to the polarization plane of the laser beam (see Figure 2), large orientation-dependent variations in signal intensity are possible. This allows determination of the orientation of specific moieties in the polypeptide relative to the fiber axis.

The amide I mode of the polypeptide backbone is particularly sensitive to the local secondary structure.[6] Conventional analysis of the amide I mode yields only a qualitative judgment of the dominant secondary structure

* To whom correspondence is to be addressed.
† Molecular Bioengineering Program, Center for Bioengineering.
‡ Department of Materials Science and Engineering.
® Abstract published in *Advance ACS Abstracts*, September 1, 1994.

0024-9297/94/2227-6177$04.50/0

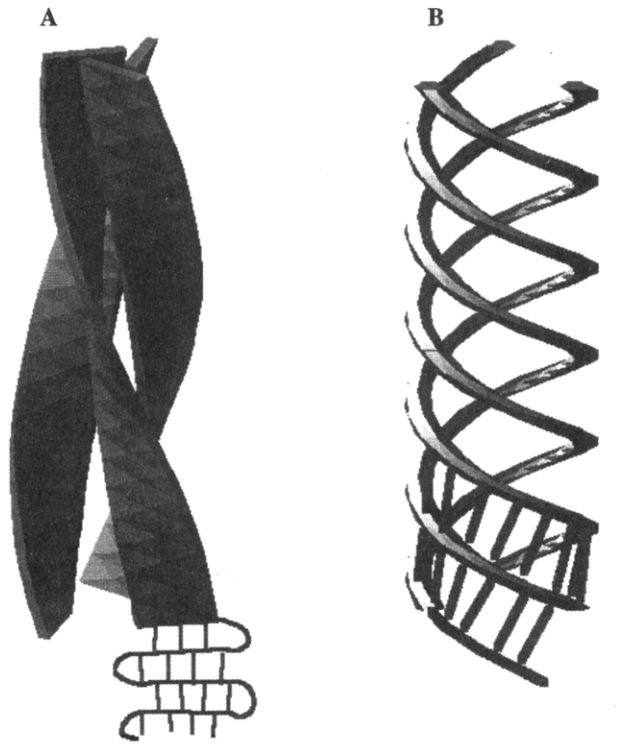

Figure 1. Two current models for the assembly of the shaft of the trimeric adenovirus fiber. Both models (which are not to scale) are triple helices, consisting of three separate polypeptide chains. In both models the hydrophobic residues are hidden within the helical interior. Model A is drawn after the modeling of O'Brien *et al.*,[1,4] which, in turn, is based on a modification of that developed by Green *et al.*[3] This model was the basis for the design of the $(Ad\ II)_{26}$ polypeptide. The model consists of three cross-β-sheet (antiparallel) ribbons twisted around each other. If all 26 repeats of the 15 amino acid sequence in $(Ad\ II)_{26}$ were intact, each ribbon would be ~250 Å long by ~20 Å wide. The three ribbons are held together primarily by the hydrophobicity of the side chains hidden by intersheet contact. Model B, which is a crude representation of that of Stouten *et al.*,[5] has no intrastrand hydrogen bonding, but only interstrand hydrogen bonds (forming a parallel β-sheet) that contribute to holding the structure together. Note that the polypeptide chain axes of the β-sheet are on average nearly perpendicular to the helix axis in the Green model, but are tilted more toward the helix axis in the Stouten model.

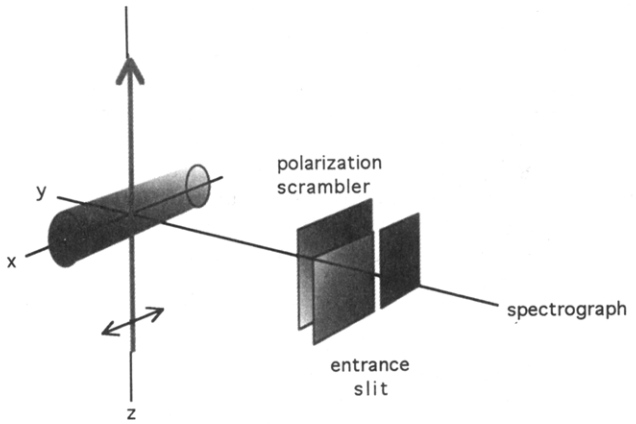

Figure 2. Schematic representation of the Raman experimental axes. The laser propagates along z and is polarized along the x-axis. Light is collected along the y-axis by a camera lens (not shown). Fibers are oriented either along x or y. Note that when the fiber is oriented along y only a small amount of the scattered light is blocked by a wire supporting the fiber.

type (α-helix, β-sheet, or random coil) based on peak frequency. However, Williams has shown that percentages of a protein's secondary structure can be estimated[7] by a non-negative least squares fit of the amide I region to a set of reference spectra. The orientation and secondary structure percentages can be used to evaluate models of $(Ad\ II)_{26}$ fiber structure.

In addition to Raman spectroscopy, we have applied optical birefringence, electron diffraction, and both optical and electron microscopies to determine the conformation and orientation of the polypeptide in the spun fibers. Silks are a useful reference for studying the structure of the $(Ad\ II)_{26}$ fiber, since the silks of both the silkworm *Bombyx mori* and the spider *Nephila clavipes* are spun from birefringent protein solutions.[8,9] The $(Ad\ II)_{26}$ results are compared with recent data from silks from the silkworm and the spider, all three of which materials appear to have similar proportions of polypeptide secondary structure.[10]

Materials and Methods

Approximately 0.5 m of $(Ad\ II)_{26}$ fiber was donated by Dr. John P. O'Brien of DuPont Fibers (Experimental Station, Wilmington, DE). The sequence of the gene was designed, the artificial gene expressed, and the polypeptide purified and spun at DuPont as described by Hoess *et al.*[2]

Bright field microscopy of the $(Ad\ II)_{26}$ fiber immersed in distilled water was performed with a Zeiss ICM 405 inverted microscope. Images were collected with an MTI DAGE Model 66 SIT camera. A Macintosh II computer equipped with a frame grabber board was used to digitize the images, which were then processed using the public domain NIH software package Image version 1.47. Transmitted polarized light microscopy was used to determine the direction and extent of molecular orientation of the $(Ad\ II)_{26}$ fibers by characterizing the sign and magnitude of the birefringence. Measurements were carried out on a Leitz Wetzlar Laborlux 12 POL microscope equipped with a strain free PL Fluotar 40× objective lens (NA = 0.70). All fiber samples were observed with orthoscopic (parallel) illumination. A Berek compensator (Leitz Tilting Compensator B) was used in green light (560 nm) to quantify the magnitude and sign of the fibers' birefringence. Ten birefringence measurements were made on each of two samples to determine the average molecular order in the fibers. Birefringence values were compared with data from the *B. mori* silk.[11]

The microstructure of the fibers was also investigated by scanning electron microscopy (SEM) and transmission electron microscopy (TEM). Segments of fibers were immersed in liquid nitrogen and either cut with a scalpel or broken by hand in tension or by bending. The fractured ends were mounted on an adhesive graphite tab for viewing in the SEM. A thin coating of Au–Pd was applied to reduce charging effects. The SEM was a JEOL 6300 field emission microscope operated at an accelerating voltage of 3 kV. For TEM, fibers were mounted in Medcast epoxy and ultramicrotomed to 60 nm sections. A Philips 430T TEM operating at 200 kV was used to examine the sections.

Raman spectroscopy of the fibers was performed with a SPEX 500M spectrograph equipped with a SPEX Spectrum-1 liquid N_2-cooled CCD detector, as described elsewhere.[10] A Lexel argon-ion laser was used for sample illumination. The principal axes of the system were designated as follows: the beam propagated along the z-axis, the y-axis was the axis of the light collection optics, and the electric vector of the laser polarization was oriented along the x-axis (see Figure 2). The fibers were soaked in 15% H_2O_2 for up to 30 min at 21 °C with periodic stirring to reduce the overwhelming luminescent background of the as-received fibers. Spectra reported were collected for 100 s from single fibers oriented along the x- or y-axes, using a laser power of ~100 mW of 514.5 nm radiation and a 20 μm slit width.

Initial processing of spectra prior to secondary structural analysis was performed with SPEX DM3000 software, version 3.12. Data collected in ~500 cm^{-1} windows were concatenated in the SPEX software and were subsequently transferred to the Macintosh software package Igor (WaveMetrics, Lake Oswego, OR) for smoothing, baseline subtraction, normalization, peak-fitting, and removal of side chain peaks interfering with the amide I band.[10] A "pseudoisotropic" spectrum was generated by averaging two of the y orientation spectra with one x orientation

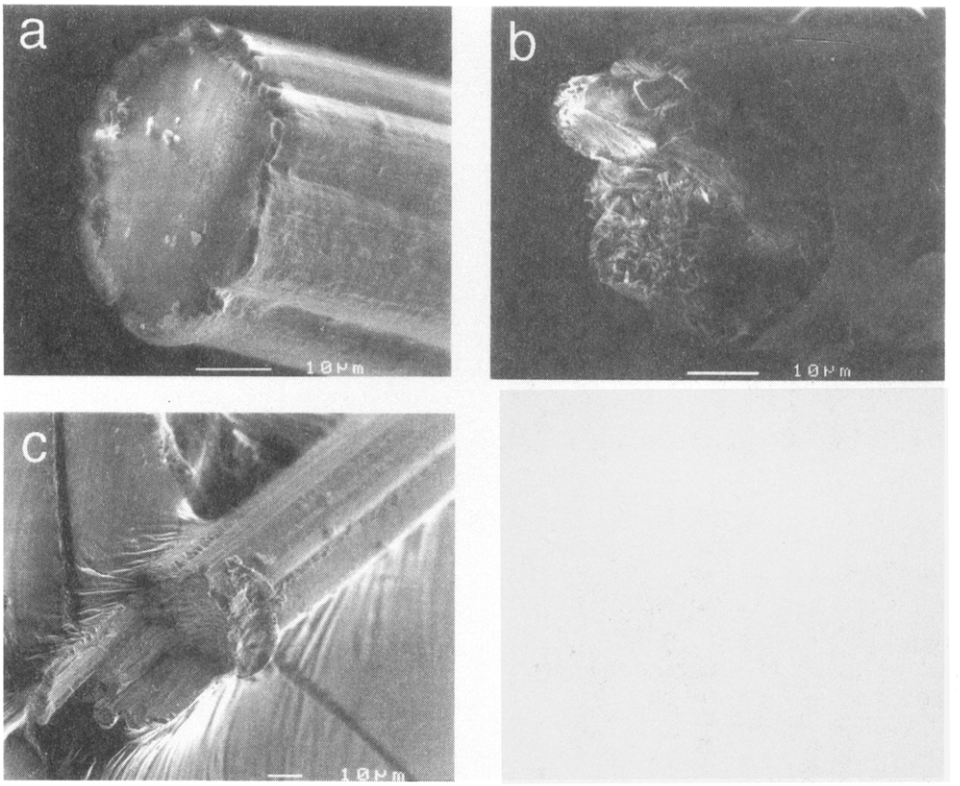

Figure 3. Three scanning electron micrographs of (Ad II)$_{26}$ fibers cut or broken to reveal internal structure and its response to damage. The fiber in (a) was cut transversely with a scalpel. The fiber in (b) was broken under tension. Debris from the spalled skin may be seen adhering to the fiber some distance behind the fracture surface. The fiber in (c) was broken by bending. Glue used to hold the fiber to the substrate can be seen on either side.

spectrum. Williams' algorithm was applied to x, y, and "pseudo-isotropic" spectra according to techniques previously described.[7,10,12]

The intensities of amide I bands in x and y orientations were used for a semiquantitative comparison of the degree of molecular orientation within the (Ad II)$_{26}$ fiber with those of *N. clavipes* dragline silk and domesticated silkworm *B. mori* silk.[10] Spectra collected in both orientations were normalized to the intensity of the C–H deformation peak at ~1450 cm^{-1}. The amide I peak area was measured after subtraction of a side peak attributed to aromatic amino acid side chains (as above). Amide I peak intensity measurements were made from the highest point in the amide I band, which varied over ~5 cm^{-1} from fiber type to fiber type.

Results

The (Ad II)$_{26}$ fiber cross-sections were roughly circular, although heavily fluted, and approximately 50 μm in diameter. However, the diameters varied by as much as a factor of 2 along a given fiber. Examination of the scalpel-sliced cross section (Figure 3a) revealed skin–core formation (the presence of distinct microstructures inside and at the surface of the fibers). This suggests long range chemical or physical segregation during processing. The skin was relatively plastic and flowed easily during tensile failure. The drawing and smoothing of the surface can be seen in the end view of the tensile fracture surface (Figure 3b). Closer examination of the core fracture surface revealed a texture typical of ductile failure, although the core was evidently not nearly as plastic as the skin layer. The fiber stressed to failure by bending is shown in Figure 3c. The compression surface at the top indicates that the fiber did not fail by kinking, which is consistent with the high compressive strength and stiffness expected for this material. The tension–compression transition region can be seen by the change in failure mode in the fracture surface. The images of sections of the fibers that failed under tension are consistent with a fibrillar substructure.

An initial concern was the possibility of a structural perturbation of the fiber caused by the H_2O_2 wash used to reduce its luminescence. No consistent changes in fiber diameter were observed, but Figure 4 illustrates a change in gross morphology consistently noted after 30 min in 15% H_2O_2; fibers washed in H_2O_2 were much smoother. However, bright field microscopy in unpolarized light did not indicate whether the skin of the fiber was removed or simply re-ordered to eliminate the fluting. The reduction in luminescence in parallel with an alteration of the fiber skin suggests that the skin initially contained the highest concentration of contaminant fluorophores.

Ten birefringence measurements were taken on each of two segments of the (Ad II)$_{26}$ fiber ~1.5 cm in length, at approximately 1 mm spacings. These measurements were repeated following peroxide treatment. The berefringences of the untreated and peroxide-treated fibers were 0.008 ● 0.001 and 0.0083 ± 0.0006, respectively. While the mean birefringence after treatment was essentially identical, the decrease in the standard deviation suggests that the peroxide treatment made the fibers more uniformly birefringent along their lengths. These experiments also suggest that the overall molecular organization within the fiber core was not significantly altered by the peroxide treatment. The fiber birefringence is very low compared with a model material such as *B. mori* silk, which has an average birefringence of 0.053.[11] As in *B. mori* silk, the higher refractive index lies along the length of the fiber. If the chemical and microstructural features of (Ad II)$_{26}$ fibers and *B. mori* silk fibers were identical, the (Ad II)$_{26}$ fibers would be clearly identified as the less oriented of the two. On the other hand, the molecular aggregates that make up the (Ad II)$_{26}$ fiber may be quite different from those in silk, and the presence of different aromatic residues can affect the birefringence. A direct comparison across materials may not be justified.

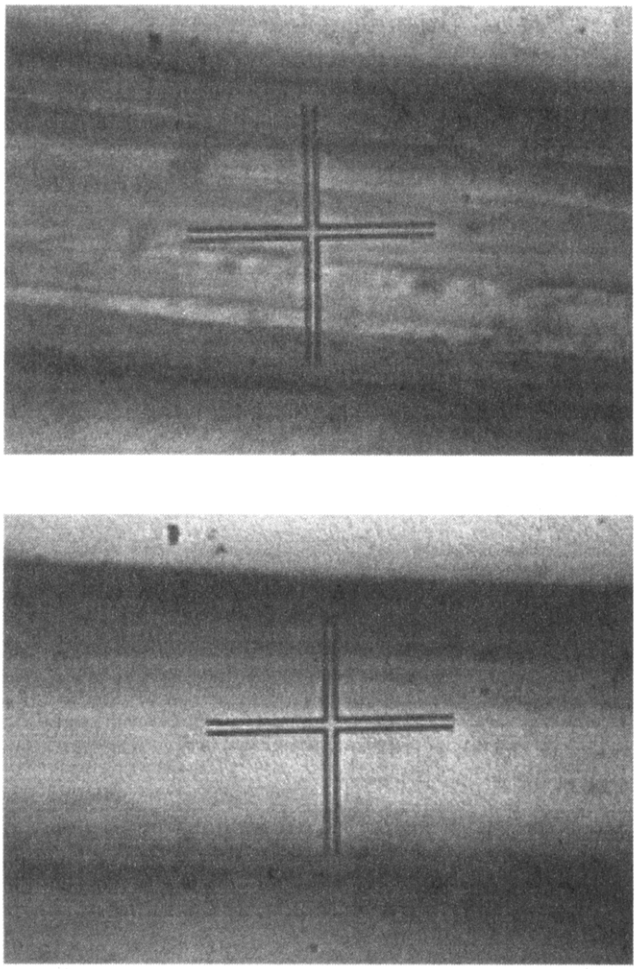

Figure 4. Bright field optical micrographs of the $(Ad\ II)_{26}$ fiber in distilled water. Above is an untreated fiber, the surface of which is covered by longitudinal ridges; below is a fiber that has lost its ridges after a 30-min soaking in 15% hydrogen peroxide. The length of the fiducial mark is 39 μm.

Transmission electron micrographs of thin sections of the $(Ad\ II)_{26}$ fiber (not shown) were featureless, indicating a complete absence of substructure or crystallinity. Only diffuse electron diffraction was observed, which is inconsistent with the presence of ordered arrays of fibrils. Although any structure present may have degraded before viewing, this is not likely as no residual physical or chemical variations were evident. These results are in sharp contrast to the evident crystallinity observable in fibers of *N. clavipes* silk treated and stored in a similar manner.[10,13]

Typical Raman spectra collected in x and y orientations from single H_2O_2-bleached $(Ad\ II)_{26}$ fibers are shown in Figure 5. The frequency of the amide I band is consistent with the existence of a large fraction of β-sheet, as expected. Note that the amide I and III band intensities are demonstrably dependent on the orientation of the fibers, but in the opposite sense; the amide I is strongest with the fiber in the y orientation, whereas the amide III is strongest with the fiber in the x orientation. This can be explained only by preferential orientation of the polypeptide backbones along the fiber axis, as seen in silks by Raman spectroscopy[10] and other techniques.[14,15] The data in Table 1 demonstrate two ways of quantifying this orientation. The peak intensity ratios emphasize those amide bonds that dominate the structure, and so are selective, in this case, for the β-sheet. The fact that the peak intensity ratio is nearer to 1 in the $(Ad\ II)_{26}$ fiber than in either *B. mori* or *N. clavipes* fibers suggests that β-strands in the $(Ad\ II)_{26}$ fiber are less aligned along the fiber axis than in these two silks. However, the peak area ratios for all three fibers are strikingly similar. The area ratios encompass contributions from amide bonds in all secondary structures, suggesting that overall order in the fibers is very similar.

Table 1. Orientation Dependence of Amide I Band Intensities (x Orientation Intensity I_x Divided by y Orientation Intensity I_y)

sample	peak intensity ratio[a]	integrated area ratio
$(Ad\ II)_{26}$	0.76	0.82
N. clavipes dragline silk	0.59	0.83
B. mori degummed silk	0.59	0.80

[a] Dominated by contributions from β-sheet domains.

Table 2. Estimation of Secondary Structure in the $(Ad\ II)_{26}$ Fiber (Estimated Error ±5%)

structural type	% x orientation	% y orientation	% "pseudo-isotropic"
ordered helix	9	0	2
disordered helix	0	0	0
β-sheet	54	61	59
β-turn	17	20	19
undefined	16	17	17
sum	97	99	97

The results of the secondary structure analyses of the amide I bands from these spectra and of the band in the "pseudoisotropic" average are displayed in Table 2. The percentage of combined parallel and antiparallel β-sheet is estimated to be as high as 59% (in the pseudoisotropic spectrum), which is consistent with the qualitative X-ray diffraction results of O'Brien *et al.*[1] The small amount of α-helix present is found in only the x orientation spectrum, and in the combination spectrum insofar as the x spectrum makes a one-third contribution. This suggests that what helical structure exists is highly aligned along the fiber axis. Furthermore, the absence of any indication of disordered helix suggests that those helices that are present are long. Neither the estimated turn content (~19%) nor the estimated undefined content varies significantly from spectrum to spectrum. At least for the random coil (or indeterminate structure) values, this consistency is to be expected; segments that are randomly oriented should show no preference for a particular fiber arrangement. Note that the values calculated for the "pseudoisotropic" $(Ad\ II)_{26}$ fiber are very similar to those found for the two different silks using Williams' method.[10] The content of β-sheet in both natural *B. mori* and *N. clavipes* (spider dragline) silk fibers was found to be $56 \pm 5\%$, and another $22 \pm 5\%$ is found to be β-turn.

It is important to note that the Raman spectroscopic secondary structure analysis technique employed relies greatly on the applicability of the basis set to the sample in question. At this point we have no other fibrous proteins in the basis set,[10] but the good correlation of the results on *B. mori* and *N. clavipes* silks with data from other techniques suggests that the method is relatively accurate. The Raman active amide modes are primarily sensitive to coupling between transition dipoles in repetitive secondary structure,[16] rather than to the ϕ and ψ angles themselves. However, such transition dipole coupling is also possible between one polypeptide strand and surrounding molecules, so the same polypeptide secondary structure in two different environments could generate two different amide I frequencies. Further work to determine the adequacy of the basis set is warranted.

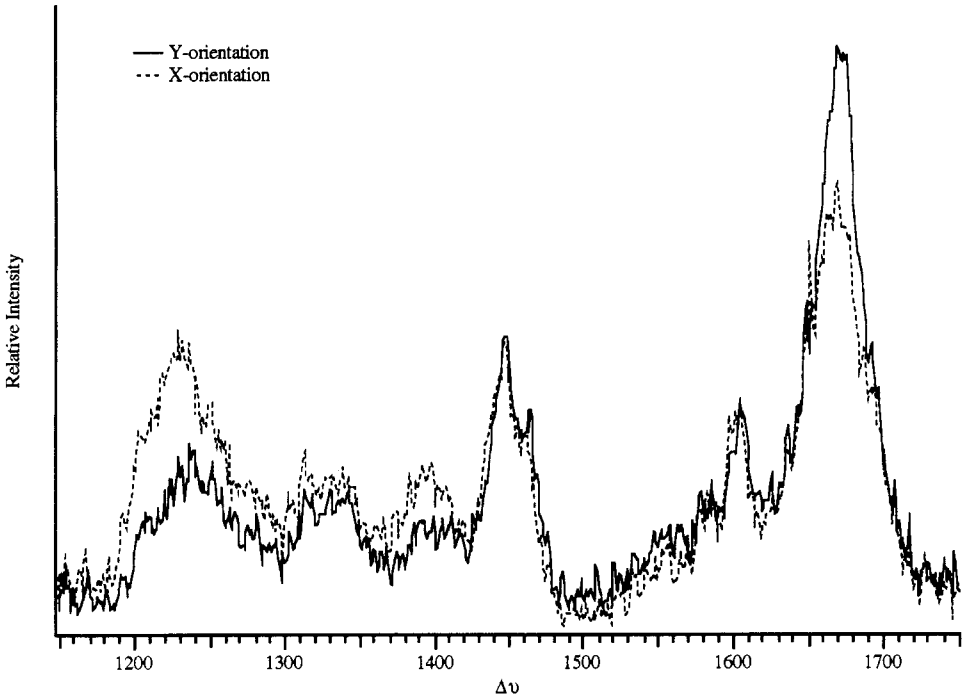

Figure 5. Overlaid Raman spectra collected from single strands of the (Ad II)$_{26}$ fiber oriented along the instrumental x and y axes. Spectra were normalized to the methylene deformation peak at ~1450 cm^{-1}. The amide I band is at about 1680 cm^{-1}, and the amide III is at about 1230 cm^{-1}. Note that the amide I is more intense in the y orientation, whereas the amide III is more intense in the x orientation, indicating some degree of alignment of the polypeptide chains along the fiber axis.

Discussion

Our data lead to the following conclusions about the structure of the (Ad II)$_{26}$ fiber:

•The polypeptide backbones of the constituent polypeptide are preferentially aligned along the fiber axis. This is an unambiguous conclusion from the Raman anisotropy measurements and is supported by comparison of birefringence measurements with those of the silk fibers.

•The dominant secondary structure present in the (Ad II)$_{26}$ fiber is antiparallel β-sheet.. This is true insofar as the existing spectral basis set allows the Williams method to correctly estimate secondary structure in fibrous proteins, which remains to be fully confirmed.

•There is no crystallinity observable by electron diffraction in the (Ad II)$_{26}$ fibers.

Because structured electron diffraction was not observed from the (Ad II)$_{26}$ fibers, we must assume that the 59% β-sheet predicted from the decomposition of the Amide I band is not assembled into crystallites as found in both *B. mori* and *N. clavipes* silk.[13] These β-sheet segments of polypeptide must exist as single strands or sheets that are too small to exhibit the long range order that would result in significant electron diffraction. While our Raman secondary structure fractions are superficially similar to those seen in both *B. mori* silk and *N. clavipes* dragline silk,[10,13] the absence of crystallinity of the (Ad II)$_{26}$ fiber, its low birefringence,[13] and low melting temperature[1] suggest that the (Ad II)$_{26}$ fiber is structurally different from the natural fibers.

Comparison with Existing Models. Green Model. O'Brien *et al.* had the trimeric Green model as the "target structure" in their synthesis of their three Ad gene constructs.[1] The Green model appears to be incompatible with our Raman data for the simple reason that the polypeptide chain orientation we find is opposite to that expected if trimers of cross-β-sheet were oriented parallel to the fiber axis. The angle of the polypeptide backbone in the Green model is nearly perpendicular to the axis of the helix. The only way in which this structure might fit the Raman data would be if the majority of the residues of the cross-β-sheet were in the turns between the β-strands (and are therefore oriented more along the ribbon axis). The fact that the peak intensity of the amide I band shows stronger orientation along the fiber axis than does the integrated area of the amide I band (see Table 1) argues that it is the β-strands themselves that are aligned along the fiber axis. The (Ad II)$_{26}$ fiber therefore cannot consist either of individual trimers of cross-β-sheet or of long fibrils of such trimers. These trimeric microstructures might be present, but either they are not oriented with the trimer axis parallel to the fiber or they represent only a small fraction of polypeptide organization within the fiber.

Stouten Model. The Stouten model may well be an improvement over the Green model for the structure of the adenovirus spike, but it is no more compatible with our Raman data for the (Ad II)$_{26}$ fiber than the Green model. At least 50% of the residues in the Stouten model are involved in an interchain parallel β-sheet hydrogen-bonding pattern. This is compatible with our quantitative decomposition of the amide I band given that this technique is not reliably able to distinguish between a parallel and antiparallel β-sheet using the current protein basis set. The tilt angle of the polypeptide in the Stouten model (26.8° for the β-strands and 17.4° for the all residues including loops between the β-strands[5]) *is* much larger than in the Green model. However, these tilts are still insufficient to account for the sign of the orientational anisotropy of the amide I data. According to Stouten *et al.* the polypeptide chains in their three-chain structure cannot be tilted further[5] because any such change (brought on by shifting the hydrogen-bonding pattern) would eliminate the space required for the hydrophobic residues in the triple helix interior. Also, the 28 Å diameter of the Stouten triple helical model[5] is insufficient to explain the >100 Å diameter fibrils observed by O'Brien *et al.*[1,4] in water. Finally, if either the Green or Stouten folding pattern was present in great abundance, the (Ad II)$_{26}$ fibers

should exhibit significant electron diffraction, which they do not.

Conclusions

In summary, Raman spectroscopy of the $(Ad\ II)_{26}$ fiber confirms that the recombinant polypeptide adopts a predominantly β-sheet conformation and forms fibers that display some degree of orientation. The ratio of turn: sheet as estimated from the Raman data for the $(Ad\ II)_{26}$ fiber is $\sim$0.3; 80% of the fiber consists of β-sheet with associated β-turn, with most of the remaining 20% of the polypeptide in an undefined or random coil conformation. Raman spectra and birefringence suggest that the polypeptide chains are preferentially aligned along the length of the fiber. The data are incompatible with either existing model for the organization of the adneovirus spike protein. The lack of detail in electron micrographs indicates that if there are any ordered domains in the $(Ad\ II)_{26}$ fiber, they are very small indeed. It is possible that the fibers consist of random coil and β-sheet segments partially aligned with the fiber axis. All the data in this study were taken on a single set of fibers prepared by wet spinning from 1,1,1,3,3,3-hexafluoro-2-propanol into a methanol coagulation bath at low draw rates. It is quite possible that modifications of the spinning conditions could produce fibers with different molecular and supramolecular structures.

Acknowledgment. This work was supported by NSF Grant No. BCS-9202007 to C.V. and P.Y. and by a grant from the Whitaker Foundation to the Center for Bioengineering. We are extremely gratefully to Dr. John P. O'Brien of DuPont for the gift of the fibers used in this study, and for informative discussions. We also thank Dr. Paul E. Schoen of the Naval Research Laboratory for useful discussions, Prof. Robert R. Williams of the Uniformed Services University of the Health Sciences for providing us with his FORTRAN code for protein secondary structural analysis, and both Christie Beacham and Christopher Bryden for assistance in modification of the FORTRAN code for use on our local computers. Also thanks to Hillary L. MacDonald, M.S.E.E., for her help in maintaining the Raman system.

References and Notes

(1) O'Brien, J. P.; Hoess, R. H.; Gardner, K. H.; Lock, R. L.; Wasserman, Z. R.; Weber, P. C.; Salemme, F. R. In *Silk Polymers: Materials Science and Biotechnology*; Kaplan, D., Adams, W. W., Farmer, B., Viney, C., Eds.; American Chemical Society: Washington, DC, 1994; Vol. 544, p 104.
(2) Hoess, R. H.; O'Brien, J. P.; Salemme, F. R. PCT Int. Appl. WO 92/09695, 1992.
(3) Green, N. M.; Wrigley, N. G.; Russel, W. C.; Martin, W. R.; McLachlan, A. D. *The EMBO J.* **1983**, *2* (8), 1357.
(4) O'Brien, J. P. *Trends Polym. Sci.* **1993**, *1* (8), 228.
(5) Stouten, P. F. W.; Sander, C.; Ruigrok, R. W. H.; Cusak, S. *J. Mol. Biol.* **1992**, *226*, 1073.
(6) Spiro, T. G.; Gaber, B. P. *Annu. Rev. Biochem.* **1977**, *46*, 553.
(7) Williams, R. W. *Methods Enzymol.* **1986**, *130*, 311.
(8) Magoshi, J.; Magoshi, Y.; Nakamura, S. *J. Appl. Polym. Sci., Appl. Polym. Symp.* **1985**, *41*, 187.
(9) Kerkam, K.; Viney, C.; Kaplan, D.; Lombardi, S. *Nature* **1991**, *349* (6310), 596.
(10) Gillespie, D. B.; Viney, C.; Yager, P. In *Silk Polymers: Materials Science and Biotechnology*; Kaplan, D., Adams, W. W., Farmer, B., Viney, C., Eds.; American Chemical Society: Washington, DC, 1994; Vol. 544, p 155.
(11) Peters, R. H. *The Chemistry of Fibers*; Elsevier: New York, 1963; Vol. 1.
(12) Williams, R. W. *J. Mol. Biol.* **1983**, *166*, 581.
(13) Thiel, B. L.; Kunkel, D. D.; Vincy, C. *Biopolymers*, in press.
(14) Asakura, T.; Kuzuhara, A.; Tabeta, R.; Saito, H. *Macromolecules* **1985**, *18*, 1841.
(15) Asakura, T.; Yeo, J.-H.; Demura, M.; Itoh, T.; Fujito, T.; Imanari, M.; Nicholson, L. K.; Cross, T. A. *Macromolecules* **1993**, *26*, 6660.
(16) Lowery, A. H.; Williams, R. W. In *Advances in Molecular Structure Research*; Hargittai, I., Hargittai, M., Eds.; JAI Press: London; Vol. 1. (in press).